**Carcinogenesis** vol.35 no.12 pp.2771–2777, 2014
doi:10.1093/carcin/bgu192
*Advance Access publication September 30, 2014*

# Human CD133-positive hematopoietic progenitor cells initiate growth and metastasis of colorectal cancer cells

**Chao Zhang[1,2,†], Chang Zhou[1,3,†], Xiao-Jin Wu[1,†], Min Yang[1], Zhao-Hui Yang[1], Han-Zhen Xiong[1], Chun-Ping Zhou[1], Yan-Xia Lu[1], Yuan Li[1] and Xue-Nong Li[1,*]**

[1]Department of Pathology, School of Basic Medical Sciences, Southern Medical University, Guangzhou 510515, Guangdong Province, China, [2]Department of Pathology, Sun Yat-Sen University Cancer Center, Guangzhou 510060, Guangdong Province, China and [3]Department of Anatomy and Histology, Guangdong Pharmaceutical University, Guangzhou 510006, Guangdong Province, China

*To whom correspondence should be addressed. Tel: +86 20 62787586; Fax: +86 20 62741646;
Email: nfydlxn@126.com

**The tumour-specific 'pre-metastatic niche' has emerged as a potential driving force for tumour metastasis and has been confirmed using mouse models of cancer metastasis. Vascular endothelial growth factor receptor-1$^+$ hematopoietic progenitor cells (HPCs) have been shown to play an important role in metastasis, forming a 'pre-metastatic niche' at designated sites for distant tumour progression. Here, CD133+ human umbilical hematopoietic progenitor cells (HUHPCs) were purified from human umbilical cord blood and expanded *in vitro*. We studied the effects of CD133+ HUHPCs on the growth and metastasis of four colorectal cancer (CRC) cell lines by using cell-to-cell co-culture. Our results revealed that CD133+ HUHPCs promoted the proliferation and invasion of CRC cells *in vitro* and enhanced tumour growth and metastasis *in vivo*. Moreover, CD133+ HUHPCs were observed in the pre-metastatic liver tissue using immunohistochemical analysis after co-injection of SW480/EGFP$^+$ cells and HUHPCs. Further experiments were therefore conducted to uncover the molecular mechanisms by which CD133+ HUHPCs influenced colon carcinogenesis and cancer progression. Extracted proteins were separated using the two-dimensional difference in gel electrophoresis technology. Among the differentially expressed proteins, mitogen-activated protein 4 kinase 4, stromal cell-derived factor-1, matrix metallopeptidase 9, calumenin, peripherin, leucine zipper, putative tumour suppressor 1 and guanidinoacetate methyltransferase attracted our attention. Western blot analysis further confirmed the differential expression of these proteins. Altogether, these results suggest that CD133+ HUHPCs may induce proliferation or metastasis of CRC cells and impact their derived proteins by providing a pre-metastatic microenvironment.**

## Introduction

Colorectal carcinoma is one of the major causes of cancer death worldwide (1). The main threats to patient survival and treatment are highly prevalent local recurrence and distant metastases, including liver, lung and bone (2,3). The prevention and treatment of these metastases remain a difficult challenge, and the fact that metastatic colorectal cancer (CRC) remains incurable has prompted studies of the factors underlying cancer progression (4). Many such studies have shown that the development of metastases is influenced by intricate interactions between CRC cells and the metastatic microenvironment (5). Stephen Paget proposed an original 'seed and soil' theory, by which the organ-preference patterns of the tumour metastasis result in interactions between the metastatic tumour cells and their specific microenvironment (6). More recently, it has been demonstrated that early changes in the microenvironment at the distant sites can be induced by the primary tumour, in a phenomenon termed 'pre-metastatic niche' formation. In that study, the physiological cells of the microenvironment were derived from the bone marrow. Tumour cells can secrete growth factors and cytokines, which can facilitate the recruitment and the mobilization of bone marrow-derived endothelial progenitor cells (7,8). Furthermore, Kaplan *et al.* (9,10) found that bone marrow-derived hematopoietic progenitor cells (HPCs) homed to tumour-specific pre-metastatic sites before the arrival of the tumour cells and that they could both attract the tumour cells and prepare the ground for the tumour cells to establish metastasis. Thus, reciprocal interactions between the primary tumour and the microenvironment at distant sites are a determinant of tumour progression.

Human hematopoietic stem and progenitor cells (HSCs and HPCs) are almost exclusively enriched in the cord blood (CB), bone marrow (BM) and mobilized peripheral blood (MPB) (11,12). The umbilical cord blood (UCB) also contains a population of hematopoietic multipotent stem cells that can be easily isolated (13,14). Circulating stem cells in the UCB, which are characterized by co-expression of the CD34 and CD133 markers display a certain degree of plasticity (15). Similar to bone marrow-derived HPCs, CD133+/CD34+ HPCs from human UCB can be further induced to differentiate into vascular endothelial cells and other types of mature cells (16,17); they can cause stem cells to migrate to vessels or to extramedullary sites and form colonies that participate in organ reconstruction (18). However, few studies have addressed the potential effect of these cells on tumour formation and progression.

In the present study, haematopoietic progenitor cells expressing CD133 and CD34 were purified from human UCB, expanded *in vitro* and co-cultured with colon carcinoma cells. We then evaluated the effect of CD133+ human umbilical haematopoietic progenitor cells (HUHPCs) on human colon cancer cells. We examined their effects on cell growth, adhesion, colony formation and cell invasion capacity *in vitro*. We administered CD133+ HUHPCs and colon cancer cells together into a mouse tumour xenograft model and further demonstrated that they could promote colon tumour growth and migration *in vivo*. We also investigated the cellular and molecular mechanisms by which the CD133+ HUHPCs formed permissive pre-metastatic niches to support CRC cell metastasis. These results indicate that CD133+ HUHPCs can form a 'pre-metastatic niche', which impacts the proliferation and invasiveness of colon cancer.

**Abbreviations:** BSA, bovine serum albumin; CRC, colorectal cancer; CALU, calumenin; 2D-DIGE, two-dimensional difference in gel electrophoresis technology; FBS, fetal bovine serum; Flt3-L, Flt3 Ligand; GAMT, guanidinoacetate methyltransferase; GFP, green fluorescent protein; H&E, haematoxylin–eosin; HPC, hematopoietic progenitor cell; HUCBC, human umbilical cord blood cell; HUHPC, human umbilical hematopoietic progenitor cell; IL-3, interleukin-3; IL-6, interleukin-6; LZTS1, leucine zipper, putative tumour suppressor 1; MACS, Magnetic Activated Cell Sorting; MAP4K4, mitogen-activated protein 4 kinase 4; MMP9, matrix metallopeptidase 9; MS, mass spectrometry; MTT, 3-(4,5-dimethylthiazol-2-yl)-2,5-diphenyltetrazolium bromide; PRPH, peripherin; SCF, stem cell factor; SDF-1, stromal cell-derived factor-1; UCB, umbilical cord blood.

† These authors contributed equally to this work.

## Materials and methods

### *Collection of cord blood*

In this experimental study, human UCB samples were collected from 16 consenting women who had a normal full-term pregnancy without any complications and had signed the testimonial form. The research protocol was approved by the Ethics Committee at Nanfang Hospital, and written consent was obtained from all mothers for the use of their samples. Cord blood samples were collected in 35–50 ml citrate phosphate dextrose adenine bags and processed within 24 h.

### *CD133+ cells separation*

Mononuclear cells were separated from the UCB using Ficoll Hypaque (GE Healthcare Pharmacia, Sweden), density centrifuged at 2500 rpm for 30 min at

25°C, and washed with phosphate buffer saline containing 5% bovine serum albumin (BSA; Stem Cell Technology, Canada). The CD133+ fraction was enriched using the Magnetic Activated Cell Sorting (MACS) method (Miltenyi Biotec, Germany) according to the manufacturer's instructions. The procedure was performed twice to obtain higher purity of the selected CD133+ cells; the remaining cells were designated CD133− human umbilical cord blood cells (HUCBCs). The purification efficiency was verified using flow cytometry (Partec PAS III, Germany) using counterstaining with the monoclonal antibodies CD133-PE (Epitomics Corporation) and CD34-FITC (Epitomics Corporation). The CD133+ HUHPCs were cultured in serum-free medium supplemented with 100 ng/ml BSA, 2 mM L-glutamine and 50 U/ml penicillin at 37°C in a humidified incubator of 5% $CO_2$. A combination of five cytokines was added: stem cell factor (SCF) (25 ng/ml), thromboietin (10 ng/ml), Flt3 Ligand (Flt3-L) (10 ng/ml), interleukin-3 (IL-3) (10 ng/ml) and interleukin-6 (IL-6) (10 ng/ml). After 8 weeks of culture, cytomorphology, flow cytometry, immunocytochemistry and immunofluorescence were used to identify stem cell characteristics.

*Colon cancer cell culture and MTT assay*

Four human CRC cell lines with different metastatic abilities were obtained from American Type Culture Collection: HCT116, SW480, SW620 and LOVO. The cells were cultured and stored according to the American Type Culture Collection instructions. The SW480 cells carrying wild-type green fluorescent protein (GFP) were constructed in our previous studies and designated SW480/EGFP$^+$ cells. All cell lines were cultured in RPMI 1640 (Hyclone, Logan, UT) supplemented with 10% fetal bovine serum (FBS) (Gibco-BRL, Invitrogen, Paisley, UK). Cell lines were cultured at 37°C in a humidified incubator of 5% $CO_2$.

CD133+ HUHPCs and CD133− HUCBCs from human umbilical cord blood were co-cultured with CRC cell lines (SW480, HCT116, SW620 and LOVO) at a ratio of 1:20 (CD133+ group and CD133− group, respectively). CRC cell lines without CD133+ or CD133− cells (Blank group) were also grown in the culture medium. Forty-eight hours after culturing, $2 \times 10^3$ cells of each group were seeded in 96-well plates. The cells were incubated for 1, 2, 3, 4, 5, 6 and 7 days. Cell proliferation was analysed using the 3-(4,5-dimethylthiazol-2-yl)-2,5-diphenyltetrazolium bromide (MTT) assay (Sigma–Aldrich, St. Louis, MO) according to manufacturer's guide. Briefly, MTT solution was added to each well at a final concentration of 5 mg/ml, and the plates were incubated at 37°C for 4 h. After incubation, 100 µl of dimethyl sulfoxide was added to each well to dissolve the formazan formed, and absorbance was measured at 490 nm using a spectrophotometer. All measurements were performed in triplicate, and the experiments were repeated three times independently.

*Plate colony formation assay*

For each group, approximately $2 \times 10^2$ cells per well were added to three wells of a 6-well culture plate. For the colony formation assay, CRC cells and hematopoietic cells were co-seeded at a 20:1 ratio. The cells were incubated at 37°C for 14 days, washed twice with phosphate buffered saline and stained with Giemsa solution. The number of colonies containing ≥50 cells was counted under a microscope plate and used in the following calculation: plate clone formation efficiency = (number of colonies/number of cells inoculated) × 100%.

*Cell invasion assay*

Cell invasion experiments were conducted using plain Matrigel-coated transwell chambers with 8-µm pores (BD Biosciences, San Jose, CA) in 24-well plates. The membrane at the bottom of the transwell chamber was evenly coated with 50 µl of Matrigel before the addition of cell suspensions. For each group, $2 \times 10^5$ cells in serum-free medium were placed into the upper compartment of the transwell chamber, and 600 µl RPMI 1640 medium containing 20% FBS was added into the lower compartment. For the invasion assay, the radio of CD133+ HUHPC or CD133− HUCBCs to CRC cells was 1:20. After culturing at 37°C for 24–48 h, the non-invasive cells were wiped off with cotton stickers. The migrating cells were stained with Giemsa and photographed under the microscope in five random visual fields (200×). Each experiment was repeated three times.

*Animal experiments*

Six-week-old female BALB/c nude mice were obtained from the Experimental Animal Centre of Southern Medical University. All animal experiments were conducted under a licence from the Regulations for the Administration of Affairs Concerning Experimental Animals and the Chinese national guideline for animal experiments, issued in 1988. All procedures involving animals and their care in this study were approved and performed by the Southern Medical University Institutional Animal Care and Use Committee (Permit Number: SCXK GUANGDONG 2010-0032). To evaluate *in vivo* tumour growth, $2 \times 10^6$ SW480/EGFP$^+$ cells mixed with $1 \times 10^5$ CD133− HUCBCs (SW480/CD133−) were injected subcutaneously into the left dorsal flank of nude mice, whereas $2 \times 10^6$ SW480/EGFP$^+$ cells mixed with $1 \times 10^5$ CD133+ HUHPCs (SW480/CD133+) were inoculated into the right flank of nude mice ($n = 4$ per group). Mouse tumour sizes were measured with a calliper from day 5 to day 23 after injection, and the tumour volume was determined as length × width$^2$ × 1/2. All the mice were then killed, and the tumours were removed and analysed using haematoxylin–eosin (H&E) staining. For the orthotropic metastasis assay, nude mice were anaesthetized and their caecum was exteriorized by laparotomy. The subcutaneous tumours of the SW480/CD133− group and the tumours of the SW480/CD133+ group were cut into small pieces and embedded into the mesentery at the tail end of the caecum ($n = 24$ per group). To explore the function of HUHPCs in forming the 'pre-metastatic niche', six mice of each group were killed on weeks 2, 4 and 6 after tumour implantation, and the livers were removed and embedded in paraffin. Consecutive sections (4 µm) were made. In addition, the protein expression of CD133 in the liver tissues was determined using immunohistochemical analysis. On week 8, the remaining six mice of each group were killed, individual organs were removed and metastatic tissues were analysed using H&E staining. Whole-body optical images were visualized to monitor primary tumour growth and the formation of metastatic lesions.

*2D-DIGE analysis and MS identification*

Conventional 2-D electrophoretic analysis and mass spectrometry (MS) identification were performed according to the manufacturer's guide. SW480 cells and SW620 cells were individually co-cultured with either CD133+ HUHPCs or CD133− HUCBCs for 48 h. Then, CD45 microbeads (Miltenyi Biotec, Germany) were used to separate the HUHPC cells from the CRC cells prior to lysis. After the separation, the SW480 cells and SW620 cells were scraped off, harvested using centrifugation (1000*g*, 15 min, 4°C) and washed twice with cold phosphate buffered saline. The cells were resuspended in 200 µl lysis buffer (7 M urea, 2 M thiourea, 4% CHAPS, 40 mM Tris base, 1% dithiothreitol) with 1% protease inhibitors. For each sample, 50 mg of protein was labelled with 400 pmol of either Cy3 or Cy5 using minimal labelling (GE Healthcare). The Cy2 fluorophore (400 pmol) was used for labelling 50 mg of an internal standard protein for each sample. The labelling was performed on ice in the dark for 30 min, and the reaction was stopped by adding 10 mM lysine. A 50 mg aliquot of Cy3- and Cy5-labelled samples was combined before mixing with 50 mg of the Cy2-labelled internal standard. The labelled proteins were separated using immobilized pH gradient strips (NL, pH 3–10, 24 cm) (GE Healthcare). Focused immobilized pH gradient strips were equilibrated and then loaded onto 12% sodium dodecyl sulfate–epolyacrylamide gels covered with Agarose. The second dimension separation was conducted with an Ettan DIGE 12 electrophoresis system (GE Healthcare). All electrophoresis procedures were performed in the dark. After sodium dodecyl sulfate–epolyacrylamide gels, the three analytical gels were scanned with a Typhoon 9410 scanner (GE Healthcare) with appropriate excitation/emission wavelengths specific for Cy2 (488/520 nm), Cy3 (532/580 nm) and Cy5 (633/670 nm). The DeCyder 5.0 software (GE Healthcare) was used for two-dimensional difference in gel electrophoresis technology (2D-DIGE) analysis according to the manufacturer's recommendation. The DeCyder differential in-gel analysis module was used for pairwise comparisons of each sample with the internal standard in each gel. The DeCyder biological variation analysis module was then used to simultaneously match all protein spot maps using the Cy3/Cy2 and Cy5/Cy2 differential in-gel analysis ratios.

The spectra were analysed for peptide mass fingerprinting using the Biotools MS software on the in-house MASCOT server (Matrix science, London, UK). The Swiss-Prot database was used for protein identification. We specified the use of trypsin as the digestion enzyme. Peptide tolerance was set at 0.2 Da, and the decoy function was used. Protein identification with a Mowse score greater than 56 was considered significant ($P < 0.05$).

*Western blotting analysis*

SW480 cells and SW620 cells individually co-cultured with HUHPCs were separated with CD45 microbeads. Cell lysis and total protein extraction were performed on ice in radio immunoprecipitation assay buffer with 1% phenylmethylsulfonyl fluoride (KeyGen, Nanjin, China). The protein content was determined using the Bradford method. After the proteins were separated using 10% sodium dodecyl sulfate–polyacrylamide gel electrophoresis and transferred onto polyvinylidene difluoride membranes (Millipore, Bedford, MA), the membranes were blocked for 1 h in Tris Buffer Saline Tween containing 5% milk powder. The membranes were then incubated overnight at 4°C with rabbit polyclonal antihuman antibodies to mitogen-activated protein 4 kinase 4 (MAP4K4), stromal cell-derived factor-1 (SDF-1), matrix metallopeptidase 9 (MMP9), calumenin (CALU), peripherin (PRPH), leucine zipper, putative tumour suppressor 1 (LZTS1) and guanidinoacetate methyltransferase (GAMT) (diluted 1:1000; Santa Cruz Laboratories, Santa Cruz, CA) and the mouse polyclonal antihuman glyceraldehyde 3-phosphate dehydrogenase antibody (diluted 1:2000; Epitomics Corporation). The membranes were washed

three times with Tris Buffer Saline Tween and incubated with the secondary antirabbit and antimouse immunoglobulin/horseradish peroxidase for 1 h at room temperature. The signals were detected using enhanced chemiluminescence (KeyGen, Nanjin, China).

*Statistical analysis*

The results of all experiments are expressed as the mean ± standard deviation (SD) of at least three independent experiments. For *in vitro* and *in vivo* studies, the analysis of variance was used to compare the values of test and control samples. Data were considered statistically significant when $P < 0.05$(*).

## Results

*CD133+ HUHPCs were collected and positively selected*

To investigate the effects of HUHPCs on the proliferation and invasion of tumour cells, we isolated CD133+/CD34+ cells from UCB using the MACS method. First, approximately (1.82 ± 0.15) × $10^7$ mononuclear cells were isolated with density centrifugation from each 35–50-ml blood sample. The CD133+/CD34+ cells were then separated with MACS. The mean ± SD of the total cell number was (1.66 ± 0.01) × $10^5$. Then, the cells were cultured in cultivation medium supplemented with growth factors (SCF, IL-3, IL-6 and Flt3-L), and the purity of the CD133+/CD34+ cells was assessed using flow cytometry. Flow cytometry analysis revealed that most CD34+ cells (82 ± 13) % also expressed CD133 (Figure 1A). Morphological characters of CD133+/CD34+ HUHPCs were observed (Figure 1B). CD133 and CD34, the markers of hematopoietic stem and progenitor cells, were also detected in the HUHPCs by immunofluorescence and immunocytochemistry (Figure 1C and D).

*CD133+ HUHPCs enhanced colon cancer cell growth and invasion* in vitro

The effects of the CD133+ HUHPCs on the proliferation, colony formation and invasion properties of colon cell lines were investigated. To examine the potential impact of HUHPCs on the growth of CRC cells, four cancer cell lines were individually co-cultured with CD133+ HUHPCs (20:1 ratio) in 96-well plates for 24 h, and their proliferation rate was then measured. As shown in Figure 2A, colon cancer cell lines co-cultured with CD133+ HUHPCs grew markedly faster than those co-cultured with CD133− HUCBCs or cultured alone ($P < 0.05$). A colony formation assay was performed to assess the long-term impact of HUHPCs on cell growth and showed enhanced proliferation properties of the four colon cancer cell lines when treated with CD133+ HUHPCs. Thus, the cells co-cultured with CD133+ HUHPCs formed more abundant and larger clones than the control cells ($P < 0.05$, Figure 2B). Changes in cell motility and invasion of the extracellular matrix are additional characteristics of metastasis. We therefore performed a transwell assay to assess the potential impact of the CD133+ HUHPCs on the movement of colon cancer cells. Our results demonstrated that in the groups of cells co-cultured with CD133+ HUHPCs, the numbers of invasive cells were significantly elevated relative to the control groups ($P < 0.05$, Figure 3A and B). Altogether, these results suggested that the proliferation and invasion abilities of colon cancer cells were regulated by the CD133+ HUHPCs.

*CD133+ HUHPCs promoted tumour growth and metastasis* in vivo

To further establish the tumour promoting effect of CD133+ HUHPCs on CRC cells, we injected into nude mice SW480/EGFP$^+$ cells co-cultured with either CD133+ HUHPCs or CD133− HUCBCs. The tumour growth curves of the SW480/CD133+ and SW480/CD133− groups in nude mice are shown in Figure 4A. Tumour growth in the SW480/CD133− group was slower than in the SW480/CD133+ group ($P < 0.05$, Figure 4A–C), further supporting the role of CD133+ HUHPCs in CRC tumourigenicity. An orthotropic metastasis assay was then conducted by implanting tiny masses of subcutaneous tumours into the caecum terminus of nude mice. To investigate the

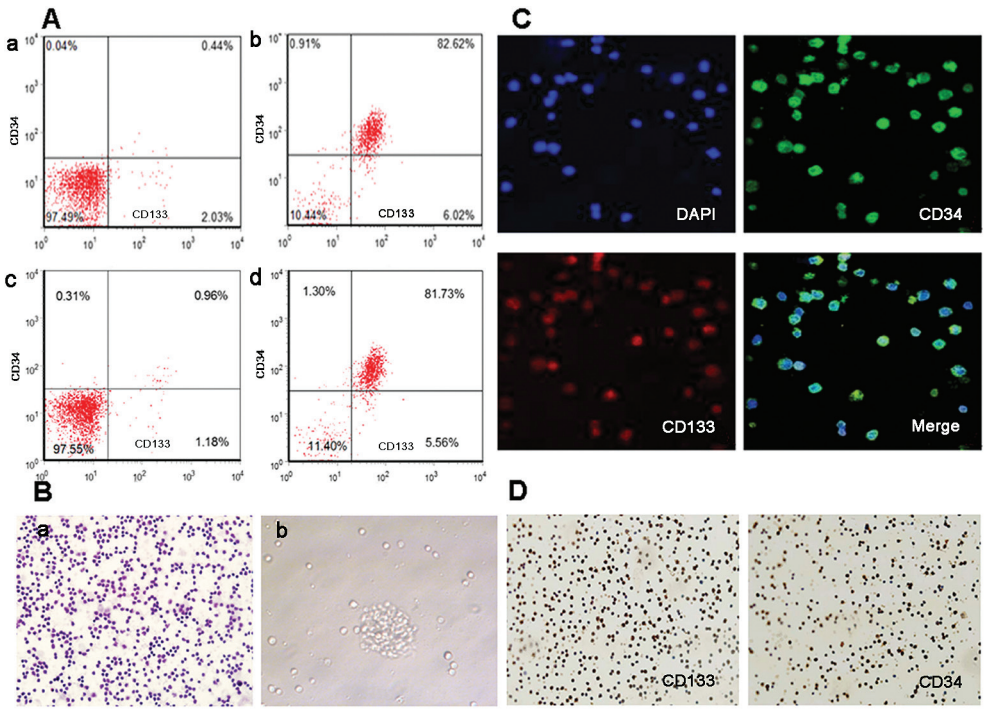


**Fig. 1.** Purification of human umbilical CD133+/CD34+ hematopoietic progenitor cells. (**A**) Flow cytometry analysis showing the percentage of HUHPCs expressing CD133/CD34 before (a) and after (b) purifying with MACS; Flow cytometry analysis showing percentage of HUHPCs expressing CD133/CD34 after culturing for 8 weeks in different expansion conditions. (c) The percentage cells cultivated in the presence of fetal bovine serum; (d) the percentage of cells cultivated in the presence of BSA. (**B**) (a) H&E staining of sorted CD133+ cells (original magnification: ×200); (b) Light images of cells in BSA (original magnification: ×400). (**C**) Immunofluorescence images of CD133+/CD34+ HUHPCs stained for 4′,6-diamidino-2-phenylindole (blue), CD34 (green) and CD133 (red) after 8 weeks of culture (original magnification: ×400). (**D**) Immunocytochemistry staining with anti-CD133 (left) and anti-CD34 (right) after 8 weeks of culture (original magnification: ×200).

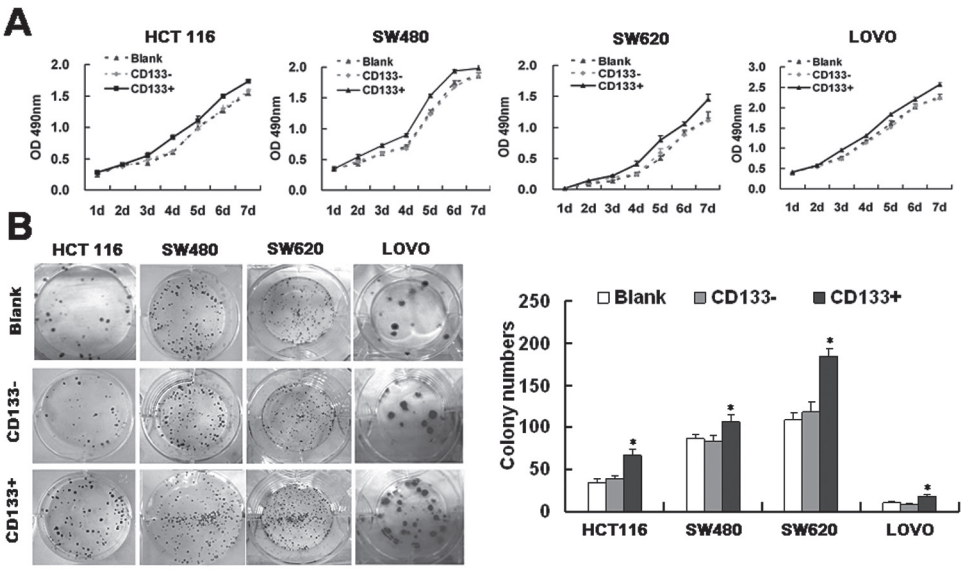


**Fig. 2.** Effect of HUHPCs on cell proliferation upon co-culturing with HCT116, SW480, SW620 and LOVO cells. (**A**) The vitality of colon cancer cells of the CD133+ group, CD133− group and Blank group was analysed using the MTT assay. (**B**) Representative images of colony formation by CRC cells 2 weeks after plating (left). The panel shows statistical data from the quantification of colony formation (right). The values shown are the means ± SD of triplicate experiments (*$P < 0.05$).

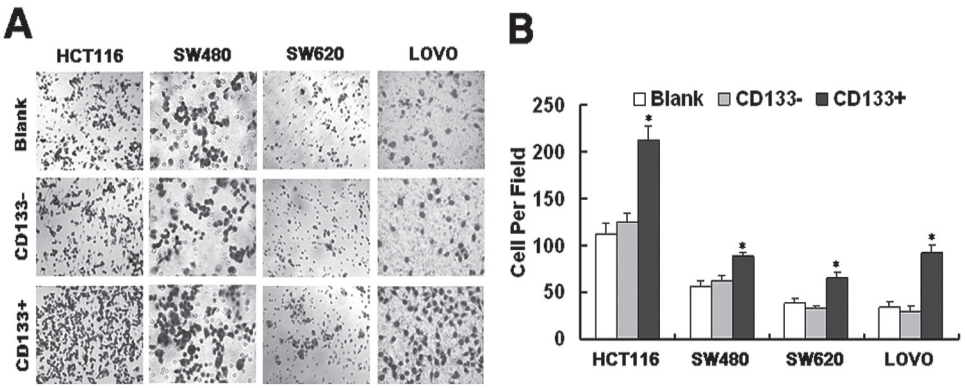


**Fig. 3.** Effect of HUHPCs on cell invasion upon co-culturing with HCT116, SW480, SW620 and LOVO cells. (**A**) The transwell assay was conducted to analyse the invasion of CRC cells. Representative fields of the migration of invasive cells on the membrane are shown (original magnification: ×200). (**B**) The average number of invasive cells per field is shown as the mean CRC cells ± SD (*$P < 0.05$).

effect of HUHPCs on forming the 'pre-metastatic niche', six mice of each group were killed on weeks 2, 4, 6, and their hepatic tissues were processed into histological sections. Immunohistochemistry results showed that the haematopoietic progenitor cells expressing the CD133 protein clustered at the shape of the periportal or vascular area only in the SW480/CD133+ group (Figure 4D). To further define the timing of HUHPC arrival, a flow cytometric analysis was conducted for the HPCs in liver tissues. Before tumour implantation, the content of vascular endothelial growth factor receptor-1$^+$ and CD133+ HUHPCs in the liver tissue was low, at less than 0.5%. From week two following tumour caecal implantation, but before the arrival of tumour cells, flow cytometric analysis demonstrated an enhanced percentage of HUHPCs co-expressing vascular endothelial growth factor receptor-1 and CD133 in mice of the SW480/CD133+ group. On the other hand, a low percentage of HUHPCs was detected in the liver tissue of the SW480/CD133− group on weeks 2, 4 and 6 following tumour implantation (Supplementary Figure 1, available at *Carcinogenesis* Online). These findings indicate that a 'pre-metastatic niche' may have been formed in the livers. To determine the effect of CD133+ HUHPCs on CRC metastasis *in vivo*, the remaining six mice of each group were killed on week 8, and their organs were subsequently scanned for metastasis using a whole-body visualization system. Visible hepatic metastasis was found in 67% (4 of 6) of the mice in the SW480/CD133+ group, whereas mice of the SW480/CD133− group showed no hepatic metastasis. The H&E staining showed metastatic lesions in the livers, distributed at the shape of the periportal area, consistent with the location of the CD133+ HUHPCs (Figure 4D). These results indicate that CD133+ HUHPCs promote tumour growth and metastasis *in vivo*.

### *CD133+ HUHPCs modulated the global protein profile in colon cells*

To assess the effect of CD133+ HUHPCs on the protein expression profiles of SW480 and SW620 cells, we applied a difference across two-dimensional DIGE proteomic approach. The soluble proteins recovered after cell lysis were labelled with the Cy3 and Cy5 dyes, and the Cy2 dye was used to label the internal standard. After 2D-DIGE, the Cy2, Cy3 and Cy5 images were scanned and analysed using the DeCyder 5.0 software. In the following software analysis, more than 1000 protein spots were detected on 2D-DIGE gels. Based on a quantitative image analysis, 16 protein spots showed a significant difference in the SW480/CD133+ group compared with the SW480/CD133− group. Figure 5A shows a representative 2D-DIGE protein map of the SW480/CD133+ and SW480/CD133− groups.

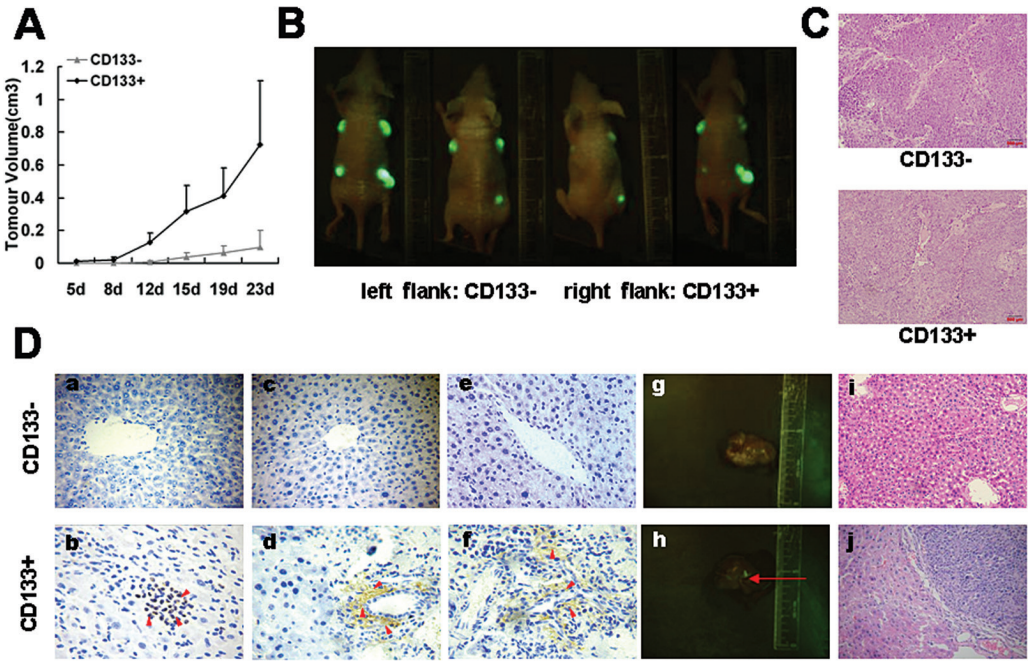


**Fig. 4.** HUHPCs promoted tumour growth and metastasis *in vivo*. (**A**) Effects of CD133+ HUHPCs and CD133− HUCBCs on subcutaneous tumour generation ($n = 4$). Tumour volume was measured every 3–4 days for 23 days. The tumour size is expressed as the mean tumour volume ± SD. (**B**) External whole-body fluorescence images of mice were captured 23 days after injection. (**C**) Representative photographs of H&E staining of primary cancer tissues are shown (magnification: ×200). (**D**) The formed tumours were implanted into the caecum terminus of other nude mice ($n = 24$). (a) Six mice of each group were first killed on week 2. CD133+ HUHPCs were not observed in the livers of the SW480/CD133− group ($n = 6$, magnification: ×400). (b) Beginning on week 2, a few CD133+ HUHPC clusters appeared in the livers of the SW480/CD133+ group before tumourigenesis ($n = 6$, magnification: ×400) (red arrows indicate CD133+ cells). (c) CD133+ HUHPCs were not observed in the livers of the SW480/CD133− group on week 4 ($n = 6$, magnification: ×400). (d) On week 4, increasing CD133+ HUHPC clusters were observed in the livers of the SW480/CD133+ group ($n = 6$, magnification: ×400) (red arrows indicate CD133+ cells). (e) CD133+ HUHPCs were still not observed in the livers of the SW480/CD133− group on week 6 ($n = 6$, magnification: ×400). (f) Dispersed CD133+ HUHPC clusters present in the livers of the SW480/CD133+ group on week 6 ($n = 6$: magnification, ×400) (red arrows indicate CD133+ cells). On week 8, the remaining six mice of each group were killed. Fluorescence images of hepatic metastases of nude mice from the SW480/CD133− group (g, $n = 6$) and SW480/CD133+ HUHPCs group (h, $n = 6$) are shown. Representative photographs of H&E staining of metastatic cancer tissues are shown for the SW480/CD133− group (i, $n = 6$, magnification: ×200) and the SW480/CD133+ HUHPCs group (j, $n = 6$, magnification: ×200).

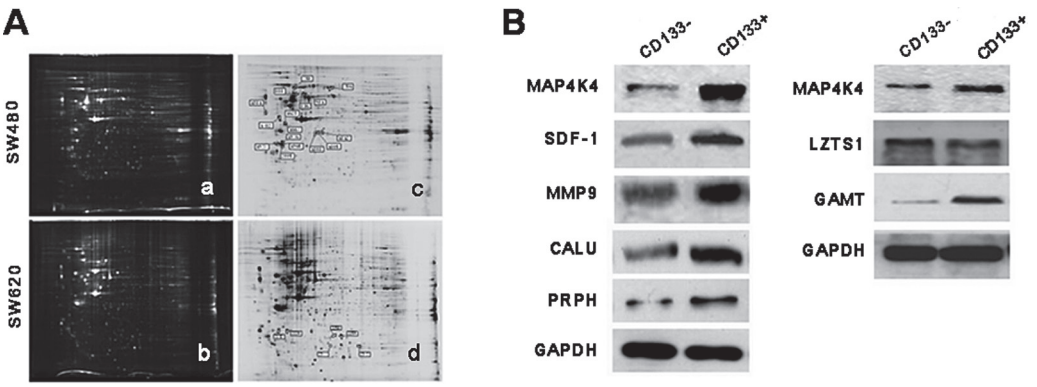


**Fig. 5.** CD133+ HUHPCs modulated the global protein profile in colon cells. (**A**) Differentially expressed proteins were identified by matrix assisted laser desorption ionization-time of flight/mass spectrometry (MALDI-TOF/MS). The distribution of all the differentially expressed protein spots in fluorescence DIGE gels is shown. (a) Merged images of the SW480/CD133− and SW480/CD133+ groups. (b) Merged images of the SW620/CD133− and SW620/CD133+ groups. Circles represent the differentially expressed protein master spots no. that had been successfully identified by MALDI-TOF/MS in SW480 cells (c) and in SW620 cells (d). (**B**) The expression of several identified proteins in SW480 (left) and SW620 (right) cells was detected using western blot analysis: MAP4K4, SDF-1, MMP9, CALU, PRPH, LZTS1 and GAMT.

Protein expression changes were considered significant only when their values exceeded the threshold settings (fold change ≥1.6, $P < 0.05$). The peptides recovered from the gel were subjected to matrix-assisted laser desorption ionization-time of flight/time of flight mass spectrometry analysis, and the MS data were submitted to a MASCOT database search, providing the identification of 16 proteins (Supplementary Table 1, available at *Carcinogenesis* Online). Western blot results showed that the expression of MAP4K4, SDF-1, MMP9, CALU and PRPH was upregulated (Figure 5B). In the SW60 cells, six protein spots were differentially expressed between the SW620/CD133+ and SW620/CD133− groups (Figure 5A, Supplementary Table 2, available at *Carcinogenesis* Online). Western blot analysis confirmed the downregulation of LZTS1 expression and the upregulation of MAP4K4 and GAMT expression (Figure 5B). Most of the differentially expressed proteins, including MAP4K4, SDF-1, MMP9 and LZTS1, are thought to be involved in central biological processes,

such as cell communication, signal transduction, cell adhesion, morphogenesis, metabolism, cell death and proliferation. Our results thus indicate that CD133+ HUHPCs might influence the cellular biological behaviour of CRC cells by regulating important intercellular proteins that are involved in various biological processes.

## Discussion

The cellular tumour microenvironment represents an essential cellular factor in the process of carcinoma metastasis. Enhanced attention has focused on the importance of both 'seed' and 'soil' for metastatic progression (19–21). This 'congenial soil' comprises a myriad of specialized cells, including fibroblasts, infiltrating cells of the immune system, endothelial cells and mural cells of blood and lymph vessels, together with their extracellular matrices, which form a supportive environment for tumour progression (22–24). The physiological cells existing in the metastatic 'microenvironment' are recruited from the bone marrow (25). In line with the 'seed and soil' hypothesis, Kaplan *et al.* postulated that bone marrow-derived HPCs are key players in initiating these early changes, creating a receptive microenvironment at designated sites for distant tumour growth and establishing the 'pre-metastatic niche'. Another study suggested that abnormally high levels of circulating HPCs (CD34+ and CD45+) are present in metastatic renal cell cancer (26). However, few experiments have addressed the role of HPCs in colon cancer. The current data prompted us to investigate the cellular and molecular cross-talk between 'seed' and 'soil' in the metastasis of CRC, and our findings highlight the importance of HPCs in the growth and metastasis of CRC cells.

In the present study, we isolated and cultured human UCB-derived HPCs expressing CD133 and CD34 *in vitro*. The trans-membrane glycoprotein CD133 was originally regarded as a cell surface marker for hematopoietic stem cells (27,28). Most of the CD133+ cells also express the membrane protein CD34. We therefore measured CD133 and CD34 expression in the UCB and selected the corresponding CD133+/CD34+ cells using flow cytometric analysis. In previous reports, FBS supplemented with a 5-cytokine combination of SCF, thromboietin, Flt3-L, IL-3 and IL-6 was used to expand CD133+/CD34+ HUHPCs. However, we found that HUHPCs growing in this culture medium maintain their stemness only for a short time and thus used BSA instead of FBS. We also observed that the majority of HUHPCs (80%) remained double-positive CD133+/CD34+ and formed stem cell clone balls throughout the expansion period of 8 weeks in basal growth medium containing BSA and the five cytokines (SCF, thromboietin, Flt3-L, IL-3 and IL-6) mixed at an appropriate ratio (10:2.5:1:1:1:1). In all cases, optimized culture medium could improve expansion, increase the amount of clonogenic HUHPCs and contribute to maintaining their stemness.

In our study, immunohistochemical analysis of human cancer progression revealed that the expression of CD133 was undetectable in the reactive lymphoid hyperplasia and in chronic tonsillitis organization tissues that were obtained from individuals without cancer, whereas CD133+ HPCs were found in metastatic lymph nodes and pre-metastatic lymph nodes from CRC patients (Supplementary Figure 2, available at *Carcinogenesis* Online). These results suggest that CD133+ HPC clusters are recruited to pre-metastatic human tissue. In view of the high expression of CD133 in metastatic cancers, we were interested in studying the role of CD133+ HUHPCs in colon cancer progression and metastasis. Our functional studies show that CD133+ HUHPCs could promote proliferation, colony formation and invasion of CRC cells *in vitro*, indicating that CD133+ HUHPCs may act as a 'tumour initiator'. Similarly, consistent with an interaction between colon cancer cells and CD133+ HUHPCs *in vitro*, the SW480/CD133+ cell group showed more notable cancer growth and metastatic foci than the SW480/CD133− group *in vivo*. Moreover, prior to the arrival of tumour cells, clusters of CD133+ HUHPCs were observed forming the 'pre-metastatic niche' in the livers. The CD133+ HUHPCs thus seem to function as 'sentinel cells' and be influenced by the local organ microenvironment and tumour cells. They may become a part of the tumour stroma and identify sites of future metastasis. Our results revealed that CD133+ HUHPCs were sufficient to promote the proliferation of CRC cells and allow the selection of CRC cell lines with a higher capacity to form liver metastasis. Altogether, these findings suggest that CD133+ HUHPCs in the tumour microenvironment play a critical role in colon cancer growth, progression and metastasis.

So far, the molecular mechanisms by which CD133+ HUHPCs influence colon carcinogenesis and cancer progression have not been well defined and have received little attention. 2D-DIGE is a new, widely used proteomic technology that can efficiently provide accurate and reproducible differential expression values for proteins in two or more biological samples (29). Therefore, 2D-DIGE coupled with MS was used here to identify molecules associated with CD133+ HUHPCs that interact with either SW480 or SW620 cells. Because CD133+ HUHPCs influenced multiple functions of CRC cells, as described above, the identification of proteins involved in colon cancer biological processes as modulated by CD133+ HUHPCs was not surprising. For some of the differentially expressed proteins in our study, the results were further confirmed using western blot analysis. One of these, MAP4K4, had been reported previously to be a protein that is highly expressed in lung cancer tissues and plays important roles in transformation, invasiveness, adhesion and cell migration (30,31). Other proteins, such as SDF-1, are upregulated in many tumours, including colorectal carcinoma tissues (32). Preliminary data indicated that SDF-1 induced MMP-2 and MMP-9 upregulation in ovarian cancer cells, which was associated with increased ovarian cancer cell proliferation and invasion (33). LZTS1 is a tumour suppressor gene that is frequently altered in human cancers of different histotypes. It was reported previously that LZTS1 is downregulated in high-grade bladder cancer and that its restoration suppresses tumourigenicity in urothelial carcinoma cells (34). LZTS1 is also downregulated in breast cancer (35). The functions of CALU, PRPH and GAMT await further study. Thus, the functional significance of CD133+ HUHPCs in tumour growth and metastasis is supported by the potential roles of some of the identified proteins. Furthermore, the proteomic results provide a basis for exploring novel potential markers for CRC initiation and metastasis and directions for further study of the role of CD133+ HUHPCs in cancer development and progression. The results also suggest novel potential markers for proteomic identification of molecular abnormalities that are important in cancer development and progression within the microenvironment.

In conclusion, our study demonstrates that CD133+ HUHPCs can initiate tumour growth and metastasis by regulating the expression of tumour proteins and suggest that these cells form the 'pre-metastatic niche' before the arrival of tumour cells. Based on these results, we think HUHPCs may act as a 'tumour messenger' or 'tumour initiator' to establish the tumour microenvironment in the process of tumour metastasis.

## Supplementary material

Supplementary Material, Tables 1 and 2 and Figures 1 and 2 can be found at http://carcin.oxfordjournals.org/

## Funding

National Natural Science Foundation of China (81272758 and 81302158, 30871156) and Natural Science Foundation of Guangdong Province (S2012010009351).

*Conflict of Interest Statement:* None declared.

## References

1. Siegel,R. *et al*. (2012) Cancer treatment and survivorship statistics, 2012. *CA Cancer J. Clin*., **62**, 220–241.
2. Edwards,B.K. *et al*. (2010) Annual report to the nation on the status of cancer, 1975–2006, featuring colorectal cancer trends and impact of interventions (risk factors, screening, and treatment) to reduce future rates. *Cancer*, **116**, 544–573.
3. Ferlay,J. *et al*. (2010) Estimates of worldwide burden of cancer in 2008: GLOBOCAN 2008. *Int. J. Cancer*, **127**, 2893–2917.

4. Liu,X. *et al*. (2011) MicroRNA-499-5p promotes cellular invasion and tumor metastasis in colorectal cancer by targeting FOXO4 and PDCD4. *Carcinogenesis*, **32**, 1798–1805.
5. Beauchemin,N. (2011) The colorectal tumor microenvironment: the next decade. *Cancer Microenviron*., **4**, 181–185.
6. Paget,S. (1989) The distribution of secondary growths in cancer of the breast. 1889. *Cancer Metastasis Rev*., **8**, 98–101.
7. Lim,C. *et al*. (2013) [Microenvironment and colorectal liver metastases angiogenesis: surgical implications]. *Bull. Cancer*, **100**, 343–350.
8. Langley,R.R. *et al*. (2011) The seed and soil hypothesis revisited–the role of tumor–stroma interactions in metastasis to different organs. *Int. J. Cancer*, **128**, 2527–2535.
9. Kaplan,R.N. *et al*. (2005) VEGFR1-positive haematopoietic bone marrow progenitors initiate the pre-metastatic niche. *Nature*, **438**, 820–827.
10. Kaplan,R.N. *et al*. (2006) Bone marrow cells in the 'pre-metastatic niche': within bone and beyond. *Cancer Metastasis Rev*., **25**, 521–529.
11. Lin,Y. *et al*. (2000) Origins of circulating endothelial cells and endothelial outgrowth from blood. *J. Clin. Invest*., **105**, 71–77.
12. Slovinska,L. *et al*. (2011) Umbilical cord blood cells CD133+/CD133– cultivation in neural proliferation media differentiates towards neural cell lineages. *Arch. Med. Res*., **42**, 555–562.
13. Pelagiadis,I. *et al*. (2012) CD133 immunomagnetic separation: effectiveness of the method for CD133(+) isolation from umbilical cord blood. *Cytotherapy*, **14**, 701–706.
14. Okamoto,O.K. *et al*. (2007) Common molecular pathways involved in human CD133+/CD34+ progenitor cell expansion and cancer. *Cancer Cell Int*., **7**, 11.
15. Pesce,M. *et al*. (2003) Myoendothelial differentiation of human umbilical cord blood-derived stem cells in ischemic limb tissues. *Circ. Res*., **93**, e51–e62.
16. Peichev,M. *et al*. (2000) Expression of VEGFR-2 and AC133 by circulating human CD34(+) cells identifies a population of functional endothelial precursors. *Blood*, **95**, 952–958.
17. Kuçi,S. *et al*. (2003) Identification of a novel class of human adherent CD34– stem cells that give rise to SCID-repopulating cells. *Blood*, **101**, 869–876.
18. Keith,W.N. (2004) From stem cells to cancer: balancing immortality and neoplasia. *Oncogene*, **23**, 5092–5094.
19. Lisanti,M.P. *et al*. (2011) Hydrogen peroxide fuels aging, inflammation, cancer metabolism and metastasis: the seed and soil also needs "fertilizer". *Cell Cycle*, **10**, 2440–2449.
20. Mathot,L. *et al*. (2012) Behavior of seeds and soil in the mechanism of metastasis: a deeper understanding. *Cancer Sci*., **103**, 626–631.
21. Wilson,C. *et al*. (2012) Seed, soil and secreted hormones: potential interactions of breast cancer cells with their endocrine/paracrine microenvironment and implications for treatment with bisphosphonates. *Cancer Treat. Rev*., **38**, 877–889.
22. Bissell,M.J. *et al*. (2001) Putting tumours in context. *Nat. Rev. Cancer*, **1**, 46–54.
23. Christofori,G. (2006) New signals from the invasive front. *Nature*, **441**, 444–450.
24. Zeisberg,E.M. *et al*. (2007) Discovery of endothelial to mesenchymal transition as a source for carcinoma-associated fibroblasts. *Cancer Res*., **67**, 10123–10128.
25. Catena,R. *et al*. (2013) Bone marrow-derived Gr1+ cells can generate a metastasis-resistant microenvironment via induced secretion of thrombospondin-1. *Cancer Discov*., **3**, 578–589.
26. Vroling,L. *et al*. (2009) Increased numbers of small circulating endothelial cells in renal cell cancer patients treated with sunitinib. *Angiogenesis*, **12**, 69–79.
27. Schlechta,B. *et al*. (2010) Ex-vivo expanded umbilical cord blood stem cells retain capacity for myocardial regeneration. *Circ. J*., **74**, 188–194.
28. Yin,A.H. *et al*. (1997) AC133, a novel marker for human hematopoietic stem and progenitor cells. *Blood*, **90**, 5002–5012.
29. Friedman,D.B. *et al*. (2004) Proteome analysis of human colon cancer by two-dimensional difference gel electrophoresis and mass spectrometry. *Proteomics*, **4**, 793–811.
30. Qiu,M.H. *et al*. (2012) Expression and prognostic significance of MAP4K4 in lung adenocarcinoma. *Pathol. Res. Pract*., **208**, 541–548.
31. Chen S. *et al*. (2014) SOX2 regulates apoptosis through MAP4K4-Survivin signaling pathway in human lung cancer cells. *Carcinogenesis*, **35**, 613–623.
32. Park,S.J. *et al*. (2012) Stromal-cell-derived factor 1-α promotes tumor progression in colorectal cancer. *J. Korean Soc. Coloproctol*., **28**, 27–34.
33. Shen,X. *et al*. (2009) The role of SDF-1/CXCR4 axis in ovarian cancer metastasis. *J. Huazhong Univ. Sci. Technolog. Med. Sci*., **29**, 363–367.
34. Baffa,R. *et al*. (2008) Fez1/Lzts1-deficient mice are more susceptible to N-butyl-N-(4-hydroxybutil) nitrosamine (BBN) carcinogenesis. *Carcinogenesis*, **29**, 846–848.
35. Chen,L. *et al*. (2009) Down-regulation of tumor suppressor gene FEZ1/LZTS1 in breast carcinoma involves promoter methylation and associates with metastasis. *Breast Cancer Res. Treat*., **116**, 471–478.

*Received November 21, 2013; revised August 5, 2014; accepted September 4, 2014*